Emergency Department Visits and Ambient Temperature: Evaluating the Connection and Projecting Future Outcomes

C. R. Lay[1] (ID), D. Mills[1] (ID), A. Belova[2], M. C. Sarofim[3] (ID), P. L. Kinney[4], A. Vaidyanathan[5], R. Jones[1], R. Hall[1], and S. Saha[5]

[1]Abt Associates, Inc., Boulder, CO, USA, [2]Language Technologies Institute, School of Computer Science, Carnegie Mellon University, PA, USA, [3]U.S. Environmental Protection Agency, Washington, DC, USA, [4]Environmental Health Analytics, Inc., Boston University School of Public Health, Boston, MA, USA, [5]Centers for Disease Control and Prevention, Atlanta, GA, USA

Abstract The U.S. Global Climate Change Research Program has identified climate change as a growing public health threat. We investigated the potential effects of changes in ambient daily maximum temperature on hyperthermia and cardiovascular emergency department (ED) visits using records for patients age 64 and younger from a private insurance database for the May–September period for 2005–2012. We found a strong positive relationship between daily maximum temperatures and ED visits for hyperthermia but not for cardiovascular conditions. Using the fitted relationship from 136 metropolitan areas, we calculated the number and rate of hyperthermia ED visits for climates representative of year 1995 (baseline period), as well as years 2050 and 2090 (future periods), for two climate change scenarios based on outcomes from five global climate models. Without considering potential adaptation or population growth and movement, we calculate that climate change alone will result in an additional 21,000–28,000 hyperthermia ED visits for May to September, with associated treatment costs between $6 million and $52 million (2015 U.S. dollars) by 2050; this increases to approximately 28,000–65,000 additional hyperthermia ED visits with treatment costs between $9 million and $118 million (2015 U.S. dollars) by 2090. The range in projected additional hyperthermia visits reflects the difference between alternative climate scenarios, and the additional range in valuation reflects different assumptions about per-case valuation.

1. Introduction

Rising greenhouse gas (GHG) concentrations will change our future climate. As a result, anticipated changes in the timing, duration, and severity of climate-related human health stressors may have far-reaching impacts (U.S. Global Change Research Program, 2016). A recent review identified several national-level studies that estimated impacts of future temperature changes on mortality in the United States but did not identify similar morbidity impact studies (Sarofim et al., 2016).

Our study aims to narrow this information gap and provide information about the potential morbidity impacts of future temperature changes. We examined the impact of daily maximum temperature on emergency department (ED) visits from May to September for three health conditions—hyperthermia, myocardial infarction (MI), and general cardiovascular disease—using insurance claims data for persons age 64 years and younger. We then used those health-temperature relationships to estimate the number of ED visits under alternative climate projections representative of 2050 and 2090 and a baseline climate representative of 1995. We evaluated the impacts while holding the population constant to isolate the impacts of a changing climate and then incorporated available U.S. county-level population projections to account for the additional impact of anticipated U.S. population growth and movement. We also monetized estimated incremental ED visits using available treatment cost data.

2. Methods

The modeling components of our study are (1) estimating the historical relationship between ED visits and ambient temperature, (2) projecting ED visits under alternative future climates and anticipated populations, and (3) monetizing incremental ED visits under the different climate scenarios and population assumptions.

2.1. Estimating the Association Between ED Visits and May–September Temperatures

2.1.1. Morbidity Data

We used ED data from the Truven Health ® Research database to model the impact of observed daily maximum temperatures on the daily risk of experiencing an ED visit. The data set includes information on health services used by a population with an employer-based health insurance plan. Available ED visit data included details on individual visits, including the date of the ED visit, the patient's age and home metropolitan statistical area (MSA), and all recorded diagnosis codes (coding uses the ninth International Classification of Disease, ICD9-CM, standard). We developed daily, MSA-specific counts of the number of ED visits among patients age 64 years and younger for specific diagnoses during the warm 1 May to 30 September season, for years 2005–2012. The conditions we considered included hyperthermia (ICD9-CM codes 992.0–992.9), general cardiovascular disease (ICD9-CM codes 460–519), and MI (ICD9-CM code 410). We imposed the age restriction to consider only visits by those age 64 and younger because of concerns with respect to the representativeness of the limited data for those age 65 and older and to minimize potential issues with the increasing availability, and presumed use, of Medicare as the primary source of health insurance for those persons. We chose not to pool the results for MSAs within a region in order to preserve potential MSA-to-MSA differences nor did we use a Bayesian updating approach. Researchers sometimes pool MSAs within regions or use Bayesian updating approaches to cluster similar MSAs and fit models (e.g., Schwartz et al., 2015); where MSA data are generally limited, this approach can greatly increase analytical power. However, the Truven data have records from MSAs that account for more than half of the U.S. population, and we chose to fit models separately for each MSA to reduce analytical complexity and incorporate potential MSA-to-MSA differences.

2.1.2. Environmental Data

We generated daily MSA-specific estimates of environmental variables that we evaluated with the ED data for years 2005–2012, using a population-weighted approach. In this approach, MSA-specific values reflect weighted average values where county-level populations are used to weight the available daily county-level estimates as each MSA is represented by a county or group of counties (Ivy et al., 2008; Vaidyanathan et al., 2013). The county-level estimates of the daily maximum ambient air temperature in degrees Fahrenheit (°F) were generated using meteorological predictions from the North American Land Data Assimilation System Phase 2 model, available at 0.125° (approximately 14 km × 14 km) spatial resolution (Mitchell et al., 2004). We used these values because they provide complete coverage for the United States. Similar daily estimates of particulate matter ($PM_{2.5}$) and ozone (O_3) for the 2005–2012 period were generated using a Bayesian space-time downscaler fusion model, developed by the U.S. Environmental Protection Agency (U.S. EPA) and its partners (Berrocal et al., 2012). The downscaler modeling approach combines output from the Community Multiscale Air Quality model with measurements from the Air Quality System, yielding air quality predictions at specific point locations. The aggregation methods for creating county-level environmental variables for temperature and the $PM_{2.5}$ and O_3 air pollution measures are described in Mirabelli et al. (2016).

2.1.3. Estimating the Relationship Between ED Visits and Daily Maximum Temperature

We linked the morbidity and environmental data by date and MSA. For each MSA and health condition, we estimated a nonlinear relationship between total daily ED visits among residents age 64 and younger, and daily maximum temperature using generalized additive models. We used the Negative Binomial Type I to model the daily ED visit counts (Anscombe, 1950). To incorporate nonlinearity in the relationship between log-ED visit rate and temperature, we modeled the effect of daily maximum temperature using a third-order, penalized P-spline (Eilers & Marx, 1996). We excluded an MSA if the modeled ED condition had (1) fewer than 20 total visits over the 2005–2012 period, or (2) only a single year of visit data. Other predictors in the final models included a weekend indicator variable and contrast-coded (Judd et al., 2017) calendar year variables. We weighted calendar year contrast codes by the average year-specific insured population (Sweeney & Ulveling, 1972; te Grotenhuis et al., 2017). As such, the model's intercept term corresponds to the log mean weekday ED visit rate in the average year at a daily maximum temperature of 0 °F. The following equations define the model that we fit separately for each MSA:

$$n_{\text{ED Visits/day}} \sim \text{Negative Binomial}(\mu, \sigma) \; \sigma \sim 1 \;\; \mu \sim \text{offset}(\log(n_{\text{Enrolled}})) + P\text{Spline}(\text{Temperature}_{\text{Max}})$$

$$+ \, \text{Weekend} + \text{Year}_{CC1} + \dots + \text{Year}_{CCnYears-1} + \text{Error} \tag{1}$$

The number of year terms (Year$_{CCnYears - 1}$) varied among the MSA models, with each model having one fewer year term than the MSA had years of data.

In the initial model testing, we identified an appropriate distribution family for ED visit counts, considered the inclusion of air pollutant concentration measures, and confirmed our choice of 20 knots for the P-spline. First, we considered three-count, data-generating processes for hyperthermia and MI in all included MSAs: Negative Binomial Type I (NB1), zero-inflated Poisson, and Negative Binomial Type II (NB2). We chose NB1 based on the tests in Vuong (1989), the Akaike information criterion values, and a visual inspection of the residuals. Second, we considered the PM$_{2.5}$ and O$_3$ concentrations for inclusion as predictors for hyperthermia and MI and found that these variables did not have a statistically significant impact on the daily ED visit counts in our data; hence, they were not included in the final model specification. We chose a P-spline specification with 20 knots to provide flexible fits over multiple MSAs. For the estimated relationships that converged, we selected those MSAs where the relationship between daily maximum temperature and ED visits was significant at the 5% level after controlling for the false detection rate (FDR). Given the time series nature of the data, we also tested for serial correlation using the Durbin-Watson test (Durbin & Watson, 1971) and for structural breaks using the Pruned Exact Linear Time algorithm by date (Killick et al., 2012) for all the estimated models. We did not find these issues in any of the MSA-specific models that converged.

We implemented all model estimation, fit assessment, and specification testing within the R modeling platform (R Core Team, 2016) using the *gamlss* R package (Rigby & Stasinopoulos, 2005) for the P-spline temperature representations. The structural break tests were carried out using the *cpt. mean* function with the *Pruned Exact Linear Time* method in the *changepoint* R package (Killick et al., 2016). FDR controls were implemented using the *p.correct* function with the *BY* method in the base *stats* R package.

2.2. Projecting ED Visits Under Future May–September Temperatures

We projected the number of average potential ED visits for May–September under a set of baseline climate conditions as well as those representative of midtwentieth and late twentieth century climate conditions. For each future period, we generated projections based on future climates modeled under two Representative Concentration Pathways (RCPs). The RCP scenarios differ in total radiative forcing in year 2100 relative to year 1750: 8.5 W/m^2 (RCP8.5) and 4.5 W/m^2 (RCP4.5), with the RCP8.5 scenario reflecting continued high emissions growth and limited efforts to reduce GHG emissions, whereas the RCP4.5 scenario reflects a global GHG emissions mitigation scenario.

2.2.1. Temperature Projections

Computational and resource constraints required that we select a subset of global climate models (GCMs) from the full suite of the fifth Coupled Model Intercomparison Project (Taylor et al., 2012) models for our evaluation. We selected and used five GCMs (CCSM4 (Gent et al., 2011; Neale et al., 2013), GISS-E2-R (Schmidt et al., 2006), CanESM2 (von Salzen et al., 2013), HadGEM2-ES (Collins et al., 2011; Davies et al., 2005), and MIROC5 (Watanabe et al., 2010)) for two reasons: (1) they encompass much of the variability in climate outcomes observed across the entire fifth Coupled Model Intercomparison Project ensemble and (2) these GCMs are independent and have been used by the scientific community for similar assessments (see supporting information; Sanderson et al., 2015a, 2015b). To provide localized climate projections and bias correct the projections to improve consistency with the historical period, we used the LOCA data set (Pierce et al., 2014, 2015; USBR et al., 2016). The LOCA downscaled data set provides daily minimum and maximum temperatures, among other climate variables, at 1/16° resolution from 2006 to 2100 (Livneh et al., 2015). Supporting information S1 provides additional details on our GCM selection process and a summary of general results from selected models for the RCP8.5 scenario.

For each of the future periods, we obtained 10 sets of temperature projections generated by each of the 5 GCMs for the RCP4.5 and RCP8.5 scenarios. Each set of temperature projections contained county-level daily maximum temperatures for a 20-year period. Data for years 2040–2059, centered on reporting year 2050, represent midcentury climate conditions; while data for years 2080–2099, centered on reporting year 2090, represent late-century climate conditions. The baseline climate conditions, representative of year 1995, are based on county-level daily maximum temperatures for 1986–2005; these baseline values do not vary across GCMs and RCPs. We selected calendar years to represent baseline, midcentury, and late-century climate conditions for consistency with the U.S. EPA's Multi-Model Framework for Quantitative Sectoral Impacts Analysis: A Technical Report for the Fourth National Climate Assessment (U.S. EPA, 2017) and to support integration with other results produced through this project (e.g., Belova et al., 2017; Wobus et al., 2017).

Finally, consistent with the description of the environmental data in section 2.1, we used the 2010 county population to develop county-based weights in order to combine available county values into daily maximum temperature projections for the MSAs in our analyses.

2.2.2. Population Projections

We obtained projected county-level populations for the population age 64 years and younger from U.S. EPA's Integrated Climate and Land Use Scenarios project (U.S. EPA, 2016). We aggregated these populations to produce population estimates for years 2010, 2050, and 2090, according to the mapping of MSAs to counties. We used Integrated Climate and Land Use Scenarios population values for 2010 to calculate baseline ED visits as they are more current and consistent with a broader climate impact research effort (e.g., Belova et al., 2017; Wobus et al., 2017).

2.2.3. Projections of the Number and Risk of ED Visits

We developed daily projections of ED visits for the outcome categories where the models for at least half of the MSAs evaluated converged; and for those MSAs for which the relationship between daily maximum temperature and ED visits was statistically significant, controlling for the FDR at 5% (see supporting information Table S1 for details).

The models described in section 2.1 predict the daily rate of ED visits given the daily maximum temperature and differentiate between weekends and weekdays. For each MSA in the analysis, we applied the fitted models to predict the daily number of ED visits (between 1 May and 30 September) using the climate data for each of the 20 years in the baseline, 2050, and 2090 periods. We included the effect of weekends versus weekdays in our projections, regardless of whether that effect was significant in an MSA. We reported average results from the 20 years of simulation for a given climate scenario from across each of the five GCMs. For ease of reporting, we then aggregated results to the climate regions incorporated in the forthcoming fourth National Climate Assessment (NCA; U.S. Global Change Research Program, 2017). Supporting information S2 identifies these regions and summarizes the states in each region. In this summary, initial results for MSAs that span two or more National Climate Assessment regions were allocated to each region based on the share of the projected MSA population in each NCA region for the given reporting year.

2.3. Monetizing Projected ED Visits

We developed alternative estimates of the medical expenditures for ED visits using data from two sources: Medical Expenditure Panel Survey (MEPS) data for 2008–2012 and Truven data for 2005–2012.

MEPS ED data include information on the date, diagnostic code (s), and all-payer expenditures associated with the visit, along with the survey weights that are needed to generate nationally representative estimates (Agency for Healthcare Research and Quality, 2017). We used the diagnostic codes of interest to select relevant ED visits, adjusted the per-visit expenditures in current dollars to their year 2015 dollar equivalent using a U.S. Bureau of Economic Analysis (BEA) indicators price index (Bureau of Economic Analysis, 2016), and then calculated nationally representative average per-ED-visit expenditures using the MEPS weights.

Truven data include information on current dollar insurance and out-of-pocket payments per ED visit. We adjusted dollar values to their year 2015 dollar equivalent using a BEA indicators price index (Bureau of Economic Analysis, 2016). For each diagnostic code category, we calculated average per-ED-visit expenditures by dividing the sum of all insurance and out-of-pocket payments for ED visits in the category by the corresponding total number of ED visits.

3. Results

In this section, we describe our findings in regard to the MSA-specific relationships between daily maximum temperature and ED visits from May through September for ED visit categories and report our projections of the number of ED visits under alternative future climate and population projections. We also present monetized estimates of the treatment cost for incremental ED visits attributable to a changing climate.

3.1. Modeling Maximum Daily Temperature and May–September ED Visits

We found a consistent, independent effect of daily maximum temperature on ED visits within MSAs for hyperthermia but not for the other ED visit categories. For hyperthermia, we observed a statistically significant relationship in results for 136 of the 151 MSAs that satisfied the data selection and convergence criteria. In contrast, temperature showed a statistically significant impact in fewer than 20 MSAs for general
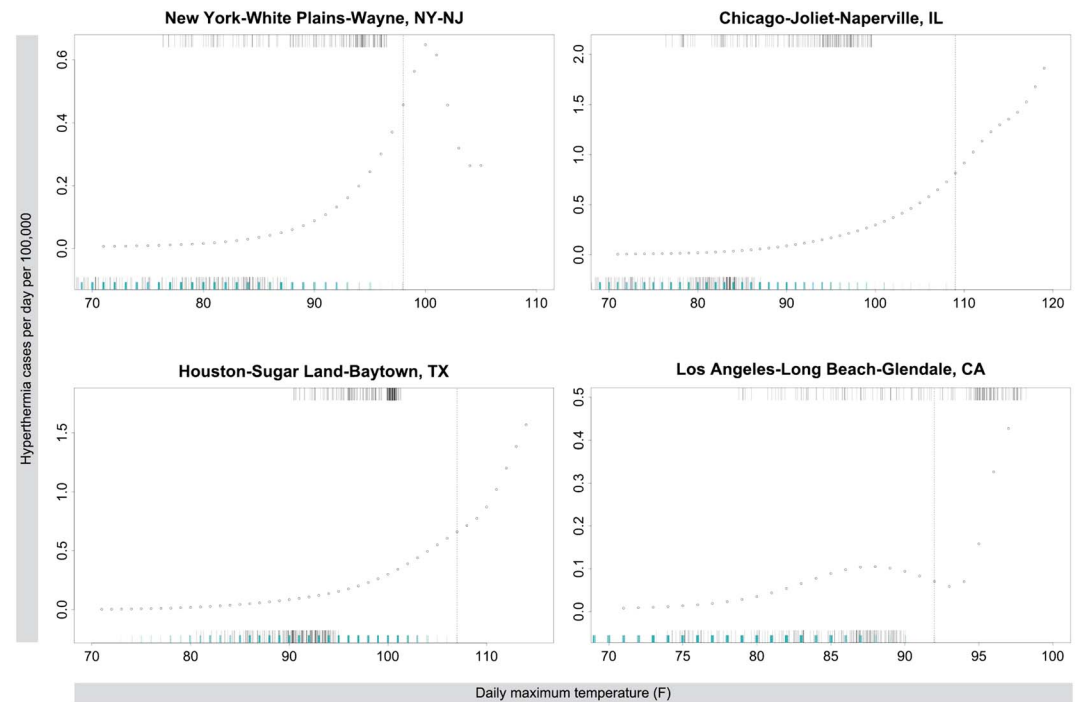
Figure 1. Fitted relationship between the daily maximum temperature and the daily hyperthermia emergency department visit rate per 100,000 individuals age 64 years and younger in select metropolitan statistical areas from May to September.

cardiovascular and MI categories from this set of MSAs; thus, we did not pursue projections for these conditions. The exclusion of patients age 65 and older from the studied population may contribute to the lack of statistical significance for these outcomes.

Figure 1 presents results from a subset of the MSAs that we developed hyperthermia ED visit projections for, which highlight a number of relationship features. In general, our modeled results in Figure 1 show increases in hyperthermia ED visits over the range of observed temperatures from the Truven data (the portion of the curve to the left of the dotted vertical line). However, in some locations, the spline fit flattened or sloped downward at the highest temperatures (e.g., Los Angeles-Long Beach-Glendale, CA). The exact shape of the relationship at the upper bounds of the observed temperatures is highly uncertain due to the limited number of observations at these temperatures.

The dotted vertical line for each MSA represents the highest daily maximum temperature observed in the 2005–2012 data for May–September. The short blue *rug* on the bottom *x* axis shows the frequency of May–September temperatures, indicated by bar thickness, used to develop the modeled temperature-ED relationship. The tall black rug on the bottom *x* axis shows the distribution of daily maximum May–September temperature for baseline year 1995, averaged by day with modeled baseline data for 1986–2005. The black rug on the top *x* axis shows the distribution of the daily maximum May–September temperature averaged by day for reporting year 2090 under RCP8.5 (we computed daily averages using data from the five GCMs for 2080–2099). The range of values on the axes vary by MSA.

For all MSAs in Figure 1, the distribution of the average daily maximum May–September temperature projected by day for 2090 under the RCP8.5 scenario (black rug of dashes at the top of the image for each location) overlaps with the similar distribution for baseline average daily maximum May–September temperature (black rug of dashes on the bottom of the image for each location). The upper bound of the day-specific average baseline temperature distribution is consistently below the upper bound from the RCP8.5 results for 2090, indicating an increase in the frequency of hot days in 2090 under the RCP8.5 scenario. This approach, averaging projected values by specific day using data from all 5 GCMs and the 20 years associated with 2090, masks some of the most extreme projected daily maximum temperature values in the data. Nevertheless, in Los Angeles-Long Beach, CA, the upper bound of this day-specific distribution representative of 2090
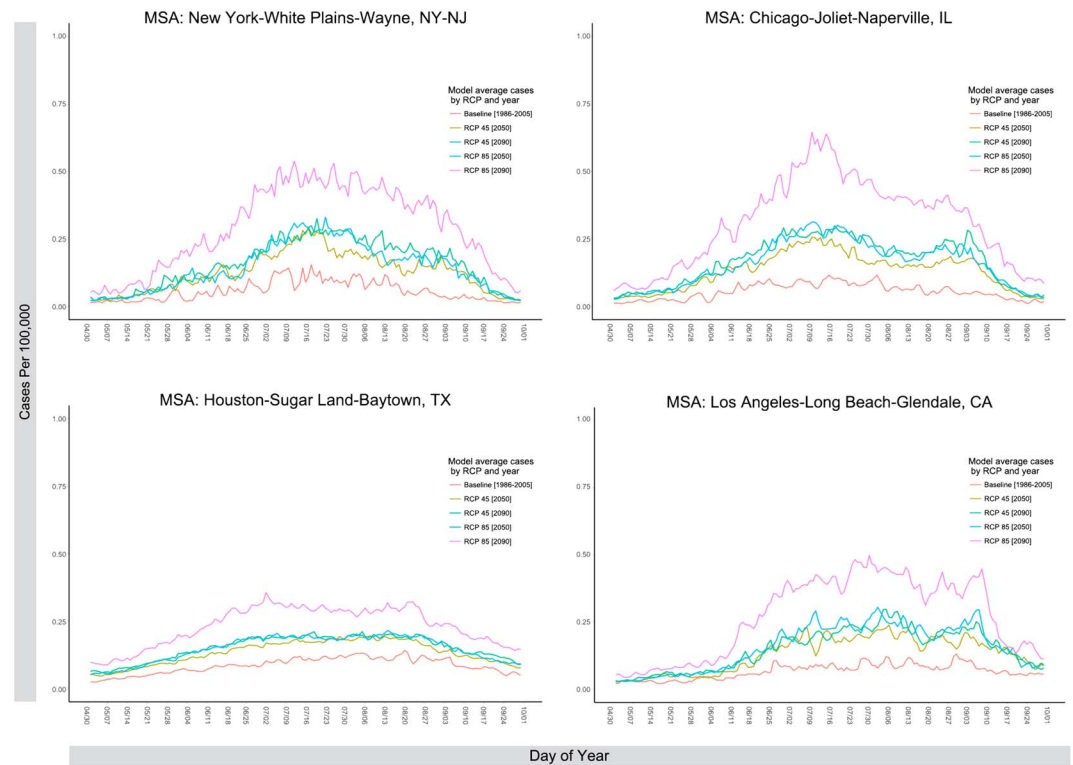
Figure 2. Projected future hyperthermia emergency department visit case rates by day averaged across global climate models under alternative climate scenarios by metropolitan statistical area (MSA). RCP = Representative Concentration Pathway.

under RCP8.5 falls outside the range of the observed daily maximum May–September temperatures from 2005 to 2012 for the MSA (i.e., values for the top black rug occur to the right of the vertical dotted line). This result indicates an anticipated dramatic warming in Los Angeles-Long Beach, CA, relative to the observed 2005–2012 period, a result observed in other MSAs as well.

3.2. Projected ED Visits for Hyperthermia

Figure 2 illustrates the distribution of projected average daily hyperthermia ED visits by day per 100,000 MSA residents age 64 years and younger for the same four MSAs presented in Figure 1 under projected baseline and future climates by RCP scenario and reporting year. For each day, the estimated number of ED visits is an arithmetic average of the results from the five GCMs and the 20 years supporting the specific reporting year.

Similarities in daily hyperthermia ED visit rate profiles across the four selected MSAs include the following:

1. ED visit rates that peak in July or August, accentuated over time for each RCP.
2. The following ordering of the results in terms of the highest rates to the lowest at almost all points in time: RCP8.5 in 2090, RCP8.5 in 2050, RCP4.5 in 2090, RCP4.5 in 2050, and the baseline period.
3. The results for the RCP4.5 scenario in 2090 and the RCP8.5 scenario in 2050, as shown by the near overlay of these lines.

Notable differences across the MSA-specific daily hyperthermia ED visit rate profiles include the timing and magnitude of peak rates and the time it takes to return from peak levels to those observed at the start of the season.

Table 1 shows the annual number of hyperthermia ED visits projected under alternative emissions scenarios and population size assumptions across all regions for specific reference years during May–September. Estimates are aggregated to the NCA regions, and represent averages over the five GCM models and the 20 years contributing to each reporting year. MSAs, where criteria for inclusion (data availability, convergence, and significance) were not met, do not contribute to the totals.

Table 1
Summary of Projected Annual May–September Hyperthermia ED Visits for Those Age 64 Years and Younger Averaged Across GCMs for RCP4.5 and RCP8.5, by NCA Region

NCA region	Baseline: 1995 climate with 2010 population	2050 climate with 2050 population	2090 climate with 2090 population	2050 climate with 2010 population	2090 climate with 2010 population
(1)	(2)	(3)	(4)	(5)	(6)
RCP4.5 emissions scenario					
Midwest	3,268	8,624	11,512	8,333	10,458
Northeast	3,543	9,367	13,341	8,719	11,128
Northern Great Plains	78	174	223	173	207
Northwest	81	185	267	179	235
Southeast	5,086	11,715	15,199	11,178	13,061
Southern Great Plains	2,050	4,637	6,395	3,673	4,202
Southwest	2,718	6,801	9,725	5,170	5,891
Total ED visits[a]	16,825	41,504	56,662	37,427	45,182
RCP8.5 emissions scenario					
Midwest	3,268	10,623	20,820	10,288	19,052
Northeast	3,543	11,066	25,138	10,346	21,042
Northern Great Plains	78	197	337	196	312
Northwest	81	233	639	225	555
Southeast	5,086	14,494	28,307	13,895	24,692
Southern Great Plains	2,050	5,345	9,949	4,242	6,578
Southwest	2,718	8,018	16,151	6,089	9,729
Total ED visits[a]	16,825	49,978	101,340	45,281	81,961

Note. ED = emergency department; GCM = global climate model; NCA = National Climate Assessment; RCP = Representative Concentration Pathway. Totals may not sum as a result of rounding for presentation.
[a]Regional results reflect the sum of impacts from the following number of distinct MSAs or MSAs that span multiple regions: Midwest = 42, northeast = 29, northern Great Plains = 2, northwest = 2, southeast = 46, southern Great Plains = 14, and southwest = 2.

Relative to baseline conditions representative of the 1995 climate with a 2010 population, population growth combined with the warming projected under the RCP4.5 scenario would result in a 2.5-fold increase in the number of hyperthermia ED visits expected for May–September by 2050 (column 3 versus column 2) and a 3.4-fold increase in these visits by 2090 (column 4 versus column 2). For the RCP8.5 scenario, reflecting uncontrolled growth in GHG emissions, we calculate a corresponding 3.0- and 6.0-fold increase in the number of hyperthermia ED visits for May–September by 2050 and 2090, respectively. The uncontrolled RCP8.5 emissions scenario produces higher estimated impacts than the RCP4.5 controlled emissions scenario in future years; these impacts are a 1.2-fold increase in 2050 and a 1.8-fold increase in 2090.

Columns 5 and 6 in Table 1 present projected hyperthermia ED visits for the future climate holding MSA populations constant at 2010 levels, allowing us to isolate the impact of the changing climate over time. As a result, we calculate that the changing climate under the RCP4.5 scenario will result in a 2.2-fold increase in the number of hypothermia ED visits by 2050 (column 5 versus column 2) and a 2.7-fold increase in these visits by 2090 (column 6 versus column 2). Under the RCP8.5 scenario, we estimate a corresponding 2.7- and 4.9-fold increase in the annual number of hyperthermia ED visits by 2050 and 2090, respectively. As shown in Table 2, the projected increases under the RCP8.5 scenario occur more rapidly, roughly achieving the same level of projected ED hyperthermia visits in 2050 as under the RCP4.5 scenario for 2090. These increases are equivalent to roughly 21,000 and 28,000 additional hyperthermia ED visits under the RCP4.5 scenario in 2050 and 2090, respectively, with corresponding increases of roughly 28,000 and 65,000 hyperthermia ED visits under the RCP8.5 scenario.

Population-weighted regional average hyperthermia ED visit rates for May–September highlight the varying baseline values and regional impacts of the emissions scenarios (Table 2). Baseline ED visit rates for hyperthermia vary among regions, and while all MSAs show steady increases in the projected ED visit rate over time for each RCP, these regional differences in rates persist. For instance, the Northern Great Plains and Northwest regions show lower hyperthermia ED visit rates in all periods. The impact of emissions mitigation under the RCP4.5 scenario constraining the warming of daily maximum temperatures is clear in the rate reductions in a number of regions from 2050 to 2090 (e.g., Southwest and Southern Great Plains). In contrast, these regions experience 200% to 247% rate increases from 2050 to 2090 under the RCP8.5 scenario.

Table 2

Projected Annual Population-Weighted Averages of Warm Season Hyperthermia ED Visit Rates per 100,000 MSA Residents Age 64 Years and Younger Under Alternative Climate Scenarios (Averaged Across GCMs) and Population Size Assumptions, by NCA Region

NCA region	1995 climate with 2010 population	2050 climate with 2050 population	2090 climate with 2090 population	2050 climate with 2010 population	2090 climate with 2010 population
(1)	(2)	(3)	(4)	(5)	(6)
RCP4.5 emissions scenario					
Midwest	10.13	25.56	31.79	25.84	32.42
Northeast	10.69	25.21	31.13	26.32	33.59
Northern Great Plains	8.45	18.66	22.28	18.66	22.27
Northwest	2.84	6.19	8.10	6.27	8.23
Southeast	14.79	32.02	36.58	32.51	37.99
Southern Great Plains	12.44	22.12	25.05	22.29	25.49
Southwest	10.23	19.97	22.88	19.45	22.17
RCP8.5 emissions scenario					
Midwest	10.13	31.49	57.49	31.90	59.07
Northeast	10.69	29.78	58.66	31.23	63.51
Northern Great Plains	8.45	21.15	33.68	21.15	33.66
Northwest	2.84	7.80	19.35	7.88	19.45
Southeast	14.79	39.62	68.12	40.41	71.82
Southern Great Plains	12.44	25.50	38.97	25.74	39.91
Southwest	10.23	23.55	37.99	22.91	36.61

Note. ED = emergency department; GCM = global climate model; NCA = National Climate Assessment; RCP = Representative Concentration Pathway.

The Figure 3 maps display MSA-level projections of average daily May–September hyperthermia ED visit rates per 100,000 persons age 64 years or younger combined with the MSA-level projection of the average daily maximum May–September temperatures under the alternative climate scenarios. In the figure, the relative magnitude of the rate is indicated by the size of the circle and the magnitude of the temperature change by the intensity of the circle color. The results in Figure 3 are averaged over the 5 GCMs and 20 calendar years for each reporting year.

Hyperthermia ED visit rates are moderately larger in warmer regions compared to cooler regions during the baseline period (Figure 3 and Table 3). In the RCP8.5 scenario, all regions except the northwest are as warm or warmer by 2090 than the warmest region in the baseline period.

3.3. Medical Treatment Cost Burden of Climate Change-Attributable Hyperthermia ED Visits

Following the process described in section 2.3, we calculated two estimates of the medical costs per hyperthermia ED visit: a MEPS-based estimate of $1,819 (in 2015 U.S. dollars, using 23 available observations) and a Truven-based estimate of $304 (in 2015 U.S. dollars, using 19,342 available observations). With these monetary inputs, we estimated that the annual climate change-attributable medical treatment costs of hyperthermia ED visits, the additional visits in a future period while holding the population at 2010 levels, are in the range of $6.3 million to $37.5 million assuming RCP4.5 scenario climate conditions in 2050, $8.6 million to $51.6 million assuming RCP4.5 scenario climate conditions in 2090, $8.6 million to $51.8 million assuming RCP8.5 scenario climate conditions in 2050, and $19.8 million to $118.5 million assuming RCP8.5 scenario climate conditions in 2090 (Table 3). The range in the monetized impact results in 2050 and 2090 reflects the difference in the MEPS and Truven-based costs per hyperthermia ED visit. Despite the scope of the health data in each of these data sets, there are a limited number of ED visits captured, particularly compared to other health outcomes, so a subset of the events can have an important impact on the average cost per-ED-visit results.

4. Discussion

We evaluated the effects of May–September temperatures on three categories of ED visits—hyperthermia, general cardiovascular disease, and MI—in a large portion of the U.S. population age 64 years and younger covered by employer-based insurance. We found statistically significant relationships for hyperthermia and used relationships modeled for individual MSAs to project potential health impacts from future changes in daily maximum temperature under alternative climate conditions on ED visits for hyperthermia from May
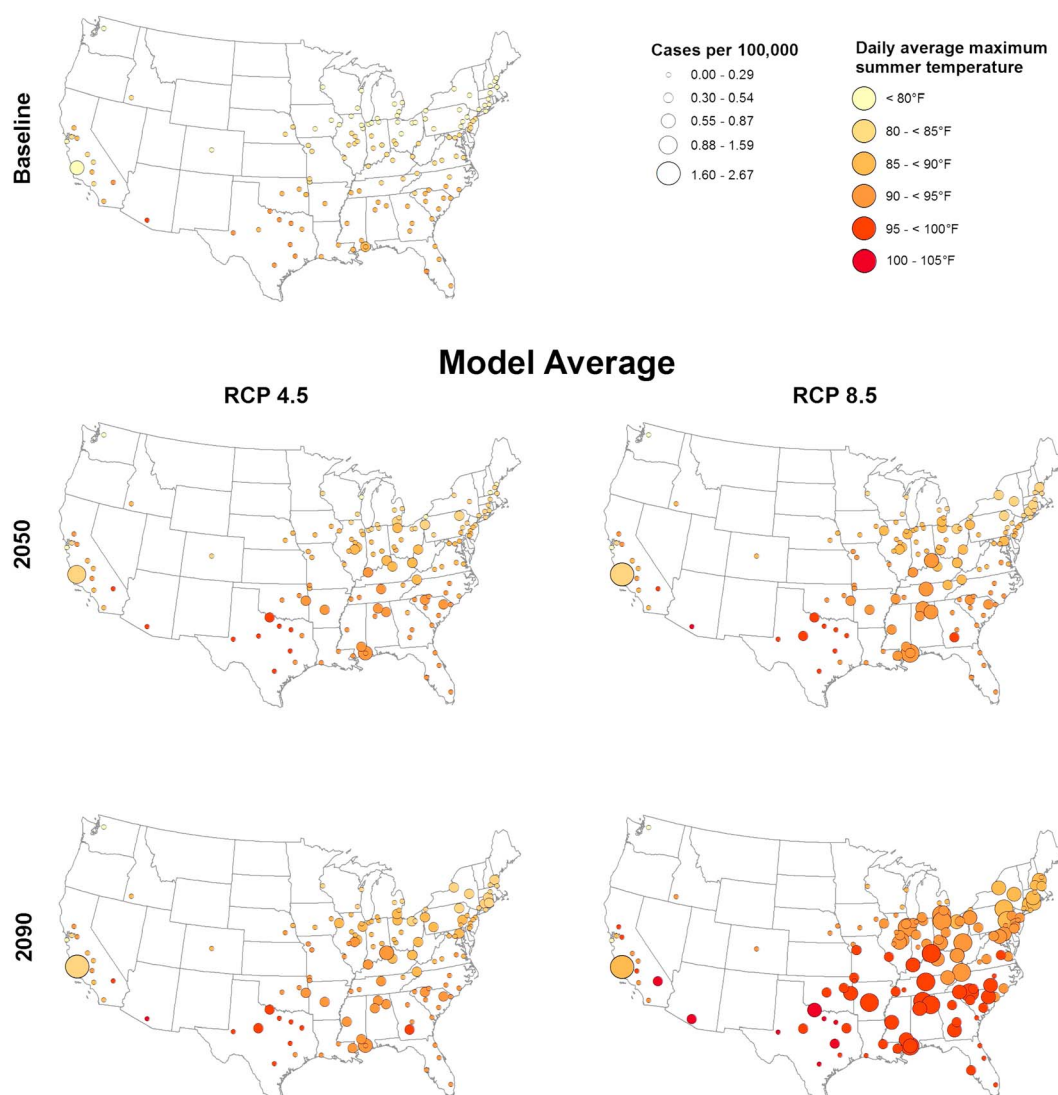
Figure 3. Projected average daily May–September maximum temperature and average daily ED visit rate for hyperthermia per 100,000 individuals age 64 years and younger for the modeled climate baseline period and each Representative Concentration Pathway (RCP) scenario and future model year. Metropolitan areas without circles did not meet our data or convergence criteria; locations not included may still experience effects.

to September. Additional work on cardiovascular endpoints may provide additional insight. For instance, the addition of daily minimum temperature may have an effect on cardiovascular ED visits, and some authors have incorporated a 3-day lag to examine the effects of long-lasting high temperature events on cardiovascular outcomes (e.g., Wang et al., 2018).

Table 3
Monetized ED Visits for Hyperthermia Attributable Solely to a Changing Climate

Incremental cases and source of the per-visit valuation estimates[a]	RCP4.5 scenario		RCP8.5 scenario	
	2050	2090	2050	2090
Incremental ED visits from anticipated climate change	20,602	28,357	28,456	65,136
Truven-based valuation of incremental visits (millions)	$6.3	$8.6	$8.6	$19.8
MEPS-based valuation of incremental visits (millions)	$37.5	$51.6	$51.8	$118.5

Note. ED = emergency department; RCP = Representative Concentration Pathway.
[a]Monetized results for representative future years are not discounted. All values are in 2015 U.S. dollars.

Table 4
Size of the Modeled Populations in the MSAs by NCA Region and Share of Total ICLUS Regional Population Age 64 Years and Younger Accounted for by the Modeled MSAs

NCA region	Number of MSAs or parts of MSAs in NCA region[a]	Population age 64 years and younger in the modeled MSAs supporting ED visit projections (millions)			Share of total NCA regional population age 64 years and younger in the modeled MSAs		
		Year = 2010	Year = 2050	Year = 2090	Year = 2010	Year = 2050	Year = 2090
Midwest	42	32.3	33.7	36.2	61%	59%	58%
Northeast	29	33.1	37.2	42.9	60%	62%	63%
Northern Great Plains	2	0.9	0.9	1.0	22%	18%	16%
Northwest	2	2.9	3.0	3.3	27%	27%	27%
Southeast	46	34.4	36.6	41.6	53%	50%	48%
Southern Great Plains	14	16.5	21.0	25.5	59%	57%	57%
Southwest	13	26.6	34.1	42.5	54%	54%	55%
Total	148	146.6	166.4	193.0	55%	54%	54%

Note. MSA = metropolitan statistical area; NCA = National Climate Assessment; ICLUS = Integrated Climate and Land Use Scenarios; ED = emergency department.
[a]Although there are 136 MSAs with statistically significant relationships for hyperthermia, several MSAs have counties in more than one NCA region and are listed multiple times in this table. For these cases, we used the projected ED visit rate for the MSA but split the case projections for that MSA population into the appropriate NCA region.

Our finding of a consistent relationship between daily maximum temperatures and hyperthermia ED visits in a large number of metropolitan areas is consistent with hyperthermia's association with exposure to high temperatures. Our finding is also consistent with results from other studies that incorporated similar data (e.g., Hess et al., 2014; Saha et al., 2015) that found a strong relationship between annual temperature anomalies and hyperthermia ED visits. Our finding of spatial variation in features of this relationship (see Figure 3 and Table 2) is also consistent with other results (e.g., Saha et al., 2015) and suggests that adaptation may play an important role, among other factors, in determining initial levels of ED visits for hyperthermia and the response to future climate conditions.

We found that with the anticipated warming from May to September under both emissions scenarios, future hyperthermia ED visits will likely increase. The magnitude of these increases is also consistent with the magnitude of the warming associated with the emissions scenario. We find that the greatest risk and the largest potential health impact in terms of additional ED visits for hyperthermia would occur under the RCP8.5 scenario in 2090. Compared to the RCP4.5 scenario, we calculated that the increased emissions under the RCP8.5 scenario would be associated with an additional 7,800 and 36,800 hyperthermia ED visits per year by 2050 and 2090, respectively, holding populations at 2010 levels (Table 2). These impacts increase, particularly for 2090, when anticipated population growth and domestic migration are taken into account. To help place our results in context, Table 4 presents information on the estimated size of the populations we address in projecting hyperthermia ED visits for years 2010, 2050, and 2090, and how our covered MSA-based populations compare to the total populations in associated NCA regions.

Table 4 shows that, with the exception of the Northern Great Plains and Northwest NCA regions, the MSAs supporting our impact projections for hyperthermia ED visits consistently account for more than half and up to two thirds of the projected total NCA regional populations for persons age 64 and younger. While the values are lower in the Northern Great Plains and Northwest NCA regions, our modeling still captures roughly one sixth to one fourth of this age group in those regions. Thus, while our projections do not capture the entire targeted population of the contiguous United States, our results generally capture more than half of the targeted population of persons age 64 years and younger in the U.S. population in 2010, 2050, and 2090.

Monetizing our projected incremental impacts attributable solely to a changing climate under different emissions scenarios provides an alternative frame of reference for consideration. Our results for this assessment found a monetized annual impact measured in millions to tens of millions of dollars in 2050 and 2090, depending on the emissions scenario and the source of estimated treatment costs per hyperthermia ED

visit. These estimates are conservative as we incorporate only payments for services incurred within the ED; costs for any subsequent treatment are not accounted for. Also, as an expenditure-based measure, these results are a conservative estimate of the true economic value of avoiding this health outcome as they do not account for lost patient or caregiver productivity associated with the ED visit or a patient's willingness to pay to avoid any pain and suffering associated with the ED visit.

However, our analysis is not without limitations. First, the Truven data do not include large segments of the population that may be vulnerable to hyperthermia and other temperature-related adverse health effects (e.g., rural residents age 64 years and younger, all persons age 65 and older, those lacking insurance, those with insurance through government agencies or programs including the Department of Defense and Medicaid). This may contribute to a conservative estimate of the morbidity associated with elevated temperatures. Additionally, as with all climate impacts projection work, many of our study locations are projected to experience large shifts in future climate conditions. This requires calculating impacts for conditions not observed in the historical data to inform the quantitative relationship we then use to project future ED visits. Perhaps most importantly, we did not attempt to quantitatively address the potential influence of adaptive measures, such as rescheduling events to avoid the hottest parts of the day, which institutions and individuals could undertake to try and influence behavior patterns to mitigate exposure to potentially dangerous conditions. These adjustments would likely decrease the total projected net impact of the anticipated impacts based on findings from similar efforts evaluating temperature-related mortality (e.g., Sarofim et al., 2016). Simultaneously, we did not consider the potential impacts of a warming climate extending the relevant season for hyperthermia beyond the May–September period or other factors that could increase future impacts (e.g., sensitivity to conditions in some regions that exceeds what we modeled). We could not explicitly examine the occupational health impacts of extreme heat, which could be important contributors to overall hyperthermia ED visits in locations where a large number of people work outdoors and are routinely exposed to high ambient temperatures.

5. Conclusion

This work represents one of the first quantitative projections of future temperature-related morbidity that addresses multiple locations across the contiguous United States. Our results thus expand the findings from a broader epidemiological literature considering the potential impact of temperature on a range of nonfatal health outcomes (e.g., Isaksen et al., 2014; Knowlton et al., 2009).

We calculate a large projected increase in ED visits for hyperthermia due to projected increases in May–September temperatures from a changing climate. With projections of increasing warming resulting in additional projected ED visits, the difference in our results for the evaluated emissions scenarios help clarify one aspect of the potential health impacts associated with alternative GHG emissions pathways. Finally, our results highlight an anticipated need for health-related agencies to continue to develop and expand health messaging, and notification and response programs to modify behavior in order to minimize future temperature-related illnesses, including ED visits for hyperthermia.

References

Agency for Healthcare Research and Quality (2017). Medical Expenditure Panel Survey, Agency for Healthcare Research and Quality. Retrieved from https://meps.ahrq.gov/mepsweb/

Anscombe, F. J. (1950). Sampling theory of the negative binomial and logarithmic distributions. *Biometrika, 37*, 358–382.

Bureau of Economic Analysis (2016). Table 1.1.9, Implicit price deflators for gross domestic product, U.S. Department of Commerce, Bureau of Economic Analysis. Retrieved from http://bea.gov/iTable/iTable.cfm?reqid=9&step=3&isuri=1&903=13#reqid=9&step=3&isuri=1&904=2000&903=13&906=a&905=2016&910=x&911=0

Belova, A., Mills, D., Hall, R., St. Juliana, A., Crimmins, A., Barker, C., & Jones, R. (2017). Impacts of increasing temperature on the future incidence of West Nile neuroinvasive disease in the United States. *American Journal of Climate Change, 6*, 166–216. https://doi.org/10.4236/ajcc.2017.61010

Berrocal, V. J., Gelfand, A. E., & Holland, D. M. (2012). Space-time data fusion under error in computer model output: An application to modeling air quality. *Biometrics, 68*(3), 837–848. https://doi.org/10.1111/j.1541-0420.2011.01725.x

Collins, W. J., Bellouin, N., Doutriaux-Boucher, M., Gedney, N., Halloran, P., Hinton, T., et al. (2011). Development and evaluation of an Earth-system model—HadGEM2. *Geoscience Model Development, 4*, 1051–1075.

Davies, T., Cullen, M. J., Malcolm, A. J., Mawson, M. H., Staniforth, A., White, A. A., & Wood, N. (2005). A new dynamical core for the Met Office's global and regional modelling of the atmosphere. *Quarterly Journal of the Royal Meteorological Society, 131*, 1759–1782.

Durbin, J., & Watson, G. S. (1971). Testing for serial correlation in least squares regression III. *Biometrika, 58*(1), 1–19. https://doi.org/10.2307/2334313

Eilers, P. H. C., & Marx, B. D. (1996). Flexible smoothing with B-splines and penalties (with comments and rejoinder). *Statistical Science*, *11*(2), 89–121.

Gent, P. R., Danabasoglu, G., Donner, L. J., Holland, M. M., Hunke, E., Jayne, S., et al. (2011). The community climate system model version 4. *Journal of Climate*, *24*, 4973–4991.

Hess, J. J., Saha, S., & Luber, G. (2014). Summertime acute heat illness in U.S. emergency departments from 2006 through 2010: Analysis of a nationally representative sample. *Environmental Health Perspectives*, *122*(11), 1209–1215. https://doi.org/10.1289/ehp.1306796

Isaksen, T. B., Yost, M., Hom, E., & Fenske, R. (2014). Projected health impacts of heat events in Washington State associated with climate change. *Reviews on Environmental Health*, *29*(1–2), 119–123. https://doi.org/10.1515/reveh-2014-0029

Ivy, D., Mulholland, J. A., & Russell, A. G. (2008). Development of ambient air quality population-weighted metrics for use in time-series health studies. *Journal of the Air & Waste Management Association*, *58*, 711–720.

Judd, C. M., McClelland, G. H., & Ryan, C. S. (2017). *Data analysis: A model comparison approach to regression, ANOVA, and beyond* (3rd ed.). New York: Routledge.

Killick, R., Fearnhead, P., & Eckley, I. A. (2012). Optimal detection of changepoints with a linear computational cost. *Journal of the American Statistical Association*, *107*(500), 1590–1598.

Killick, R., Haynes, K., & Eckley, I. A. (2016). Changepoint: Methods for changepoint detection, R package version 2.2.2. Retrieved from https://cran.r-project.org/package=changepoint

Knowlton, K., Rotkin-Ellman, M., King, G., Margolis, H. G., Smith, D., Solomon, G., et al. (2009). The 2006 California heat wave: Impacts on hospitalizations and emergency department visits. *Environmental Health Perspectives*, *117*(1), 61–67. https://doi.org/10.1289/ehp.11594

Livneh, B., Bohn, T., Pierce, D., Munoz-Arriola, F., Nijssen, B., Vose, R., et al. (2015). A spatially comprehensive, hydrometeorological data set for Mexico, the U.S., and Southern Canada 1950–2013. *Scientific Data*, *2*, 150042. https://doi.org/10.1038/sdata.2015.42

Mirabelli, M. C., Vaidyanathan, A., Flanders, W. D., Qin, X., & Garbe, P. L. (2016). Outdoor $PM_{2.5}$, ambient air temperature, and asthma symptoms in the past 14 days among adults with active asthma. *Environmental Health Perspectives*, *124* (12), 1882–1890. https://doi.org/10.1289/EHP92

Mitchell, K. E., Lohman, D., Houser, P. R., Wood, E. F., Schaake, J. C., Robock, A., et al. (2004). The multi-institution North American Land Data Assimilation System (NLDAS): Utilizing multiple GCIP products and partners in a continental distributed hydrological modeling system. *Journal of Geophysical Research*, *109*, D07S90. https://doi.org/10.1029/2003JD003823

Neale, R. B., Richter, J., Park, S., Lauritzen, P. H., Vavrus, S. J., Rasch, P., & Zhang, M. (2013). The mean climate of the Community Atmosphere Model (CAM4) in forced SST and fully coupled experiments. *Journal of Climate*, *26*, 5150–5168.

Pierce, D. W., Cayan, D. R., Maurer, E. P., Abatzoglou, J. T., & Hegewisch, K. C. (2015). Improved bias correction techniques for hydrological simulations of climate change. *Journal of Hydrometeorology*, *16*, 2421–2442. https://doi.org/10.1175/JHM-D-14-0236.1

Pierce, D. W., Cayan, D. R., & Thrasher, B. L. (2014). Statistical downscaling using localized constructed analogs (LOCA). *Journal of Hydrometeorology*, *15*(6), 2558–2585.

R Core Team (2016). *The R project for statistical computing*. Vienna, Austria: R foundation for statistical computing. Retrieved from https://www.r-project.org/

Rigby, R. A., & Stasinopoulos, D. M. (2005). Generalized additive models for location, scale and shape (with discussion). *Applied Statistics*, *54*(3), 507–554.

Saha, S., Brock, J. W., Vaidyanathan, A., Easterling, D. R., & Luber, G. (2015). Spatial variation in hyperthermia emergency department visits among those with employer-based insurance in the United States—A case-crossover analysis. *Environmental Health*, *14*, 20. https://doi.org/10.1186/s12940-015-0005-z

Sanderson, B., Knutti, R., & Caldwell, P. (2015a). Addressing interdependency in a multi-model ensemble by interpolation of model properties. *Journal of Climate*, *28*(13), 5150–5170. https://doi.org/10.1175/JCLI-D-14-00361.1

Sanderson, B., Knutti, R., & Caldwell, P. (2015b). A representative democracy to reduce interdependency in a multimodel ensemble. *Journal of Climate*, *28*, 5171–5194. https://doi.org/10.1175/JCLI-D-14-00362.1

Sarofim, M. C., Saha, S., Hawkins, M. D., Mills, D. M., Hess, J., Horton, R., et al. (2016). Temperature-related death and illness. In *The impacts of climate change on human health in the United States: A scientific assessment* (pp. 43–68). Washington, DC: U.S. Global Change Research Program. https://doi.org/10.7930/J0MG7MDX

Schmidt, G. A., Ruedy, R., Hansen, J. E., Aleinov, I., Bell, N., Bauer, M., et al. (2006). Present-day atmospheric simulations using GISS ModelE: Comparison to in situ, satellite, and reanalysis data. *Journal of Climate*, *19*, 153–192.

Schwartz, J. D., Lee, M., Kinney, P. L., Yang, S., Mills, D., Sarofim, M., et al. (2015). Projections of temperature-attributable deaths in 209 U.S. cities using a cluster-based Poisson approach. *Environmental Health*, *14*, 85. https://doi.org/10.1186/s12940-015-0071-2

Sweeney, R., & Ulveling, E. F. (1972). A transformation for simplifying the interpretation of coefficients of binary variables in regression analysis. *The American Statistician*, *26*(5), 30–32.

Taylor, K. E., Stouffer, R. J., & Meehl, G. A. (2012). An overview of CMIP5 and the experiment design. *Bulletin of the American Meteorological Society*, *93*, 485–498. https://doi.org/10.1175/BAMS-D-11-00094.1

te Grotenhuis, M., Pelzer, B., Eisinga, R., Nieuwenhuis, R., Schmidt-Catran, A., & Konig, R. (2017). When size matters: Advantages of weighted effect coding in observational studies. *International Journal of Public Health*, *62*(1), 163–167. https://doi.org/10.1007/s00038-016-0901-1

U.S. EPA (2016). Updates to the demographic and spatial allocation models to produce Integrated Climate and Land Use Scenarios (ICLUS) (Version 2) (External Review Draft), EPA/600/R-14/324. Washington, DC: U.S. Environmental Protection Agency.

U.S. EPA. (2017). Multi-model framework for quantitative sectoral impacts analysis: A technical report for the fourth National Climate Assessment, EPA/430/R-17/001. Washington, DC: U.S. Environmental Protection Agency. https://doi.org/10.13140/RG.2.2.14466.79045

USBR, NCAR, USGS, LLNL, SCU, Climate Analytics Group, et al. (2016). Downscaled CMIP3 and CMIP5 climate and hydrology projections — addendum. Release of downscaled CMIP5 climate projections (LOCA) and comparison with preceding information. Last modified October. U.S. Bureau of Reclamation, National Center for Atmospheric Research, Lawrence Livermore National Library, Santa Clara University, Climate Analytics Group, Cooperative Institute for Research in Environmental Sciences, Climate Central, U.S. Army Corps of Engineers, and Scripps Institution of Oceanography. Retrieved from http://gdo-dcp.ucllnl.org/downscaled_cmip_projections/dcpInterface.html

U.S. Global Change Research Program (2016). In A. Crimmins, J. Balbus, J. L. Gamble, C. B. Beard, J. E. Bell, D. Dodgen, et al. (Eds.), *The impacts of climate change on human health in the United States: A scientific assessment*. Washington, DC: U.S. Global Change Research Program. https://doi.org/10.7930/J0R49NQX

U.S. Global Change Research Program (2017). NCA4 chapters, U.S. Global Change Research Program. Retrieved from http://www.global-change.gov/content/nca4-outline

Vaidyanathan, A., Dimmick, W. F., Kegler, S. R., & Qalters, J. R. (2013). Statistical air quality predictions for public health surveillance: Evaluation and generation of county level metrics of $PM_{2.5}$ for the environmental public health tracking network. *International Journal of Health Geography*, *12*(1), 12. https://doi.org/10.1186/1476-072X-12-12

von Salzen, K., Scinocca, J. F., McFarlane, N. A., Li, J., Cole, J. N., Plummer, D., et al. (2013). The Canadian fourth generation atmospheric global climate model (CanAM4). Part I: Representation of physical processes. *Atmosphere-Ocean*, *51*, 104–125.

Vuong, Q. H. (1989). Likelihood ratio tests for model selection and non-nested hypotheses. *Econometrica: Journal of the Econometric Society*, *57*(2), 307–333.

Wang, Y., Nordio, F., Nairn, J., Zanobetti, A., & Schwartz, J. D. (2018). Accounting for adaptation and intensity in projecting heat wave-related mortality. *Environmental Research*, *161*, 464–471.

Watanabe, M., Suzuki, T., O'ishi, R., Komuro, Y., Watanabe, S., Emori, S., et al. (2010). Improved climate simulation by MIROC5: Mean states, variability, and climate sensitivity. *Journal of Climate*, *23*, 6312–6335.

Wobus, C., Small, E. E., Hosterman, H., Mills, D., Stein, J., Rissing, M., et al. (2017). Projected climate change impacts on skiing and snowmobiling: A case study of the United States. *Global Environmental Change*, *45*, 1–14. https://doi.org/10.1016/j.gloenvcha.2017.04.006